ELSEVIER

Thermochimica Acta 324 (1998) 15–23

thermochimica acta

An investigation of the evaporation of stearic acid using a simultaneous TG-DTA unit

Supaporn Lerdkanchanaporn, David Dollimore*

College of Pharmacy and Department of Chemistry, The University of Toledo, Toledo, OH 43606, USA

Abstract

The heat treatment of stearic acid shows a zero-order process which is in accord with an evaporation process. In this study, the melting points of three samples of stearic acid (A, B, and C) from the rising temperature experiments at the heating rate (β) of 2–12°C min^{-1} are found to be in the range of 57.4–73.5°C and that of stearic acid B in N_2 flow rate ranging from 50 to 1000 ml min^{-1} is 69.0–70.0°C. From the DTA signals, the β of 6–8°C min^{-1} and an N_2 flow rate of 100 ml min^{-1} were found to be the optimum conditions for the evaporation process of these materials. The enthalpy of vaporization (ΔH_{vap}) of stearic acid is calculated by the use of the Antoine [1] and Clausius–Clapeyron equations [2]. These ΔH_{vap} values are equal to 115.7 and 81.6 kJ mol^{-1} for the temperature ranges of 349–415 and 457–649 K, respectively. These values can be compared to the activation energy (E_{act}) which is in the range of 87.0 to 101.1 kJ mol^{-1} determined from the rising temperature experiments of three types of stearic acid subjected to various experimental conditions. Generally, $E_{act} \geq \Delta H_{vap}$. It is predicted, and verified experimentally, that the equilibrium vapor pressure and the coefficient of vaporization have a logarithmic relationship.

Keywords: Evaporation; TG; Stearic acid; DTG

1. Introduction

Stearic acid has been used as a lubricant [3], in a tablet dosage form. Pharmaceutical-grade stearic acid is not a single entity but a mixture of mainly stearic acid and palmitic acid. The United States Pharmacopoeia and The National Formulary [4] states that pharmaceutical-grade stearic acid contains not less than 40% stearic acid and that the sum of both the above compounds should not be <90%. As reported in the literature [5], the melting point and the boiling point are noted at 69–70° and 383°C, respectively. However, the boiling point is rarely observed as evaporation is often complete by this temperature. Stearic acid also slowly volatilizes at 90–100°C. Therefore, the amount of stearic acid in a tablet dosage form may vary due to evaporation during the tableting process, hence depleting its lubricating property in a given formulation.

In a moderate pressure range, the Antoine equation [2] can be written as:

$$\ln P_s = a - \frac{b}{T + c} \quad (1)$$

where P_s is the vapor pressure, T the temperature in Kelvin, a=2.303A, b=2.303B, and c=C. Here, A, B and C are the Antoine constants at a given temperature range recorded in the book by Stephenson and Malanowski [1]. It is used to determine the temperature dependence of vapor pressure. The enthalpy of vaporization (ΔH_{vap}) can be calculated from the following:

*Corresponding author. Tel.: +1-419-530-2109; fax: +1-419-530-4033; e-mail: ddollim@uoft02.utoledo.edu

0040-6031/98/$ – see front matter
PII: S0040-6031(98)00519-X

$$\Delta H_{vap} = \frac{RbT^2}{(T+c)^2} \quad (2)$$

where R is the molar gas constant=8.3145 J mol^{-1} K^{-1}.

Calculation of Δ_{vap} *for stearic acid from* Eq. (2) gives;

1. *In the temperature range=349–415 K (76–142°C)*
   [Antoine constants: A=6.17126, B=2157.5, C=−153.78, average temperature (T)=382 K (109°C)]

   $$\Delta H_{vap} = 115.7\,kJ\,mol^{-1}$$

2. *In the temperature range=457–649 K (184–376°C)*
   [Antoine constants: A=5.85188, B=1717.93, C=−201.829, average temperature (T)=553 K (280°C)]

   $$\Delta H_{vap} = 81.6\,kJ\,mol^{-1}$$

The values of ΔH_{vap} calculated above are used to compare with the E_{act} obtained from the experimental data in this study. The E_{act} can be calculated from a slope of the plot of $\ln k$ vs. $1/T$, according to the Arrhenius equation as follows:

$$\ln k = \ln Z - \frac{E_{act}}{RT} \quad (3)$$

where: k is the coefficient of evaporation per unit area (mg min^{-1} cm^{-2})=(dw/dt)×(1/∀), ∀ being the cross-sectional area of the crucible=0.294 cm^2, and Z the pre-exponential parameter.

2. Experimental

2.1. Materials

Stearic acid was obtained from three different sources, varying in the amount of stearic acid present. First of all, *99% pure stearic acid*, fine flakes (lot # 49F8449) purchased from Sigma was used as received. This material was stored in a refrigerator at a temperature of ca. 8°C. Next, *stearic acid*, *USP/NF grade*, flakes (lot # HH307) obtained from Spectrum was ground before testing. Lastly, *stearic acid*, *powder*, *food grade* (lot # 2232K) received from Pharmacia & Upjohn was tested without any treatment. For simplicity sake, these materials will be referred to as stearic acids A, B, and C in the order described above. Among these compounds, stearic acid A has the highest and stearic acid C the lowest purity.

2.2. Equipment

The SDT 2960, simultaneous TGA-DTA, TA Instrument, with the thermal analyst 2000, TA operating system version 1.0B was employed to investigate the evaporation behavior of stearic acid. An electronic flowmeter from J&W Scientific, model ADM 1000 was used to regulate the flow of purge gas through the samples.

2.3. Procedure

Two types of experimental conditions were set.

(a) *Varying the heating rate*: Nitrogen gas at 99% purity was used in all experiments. A constant flow rate of 100 ml min^{-1} was maintained throughout the experiment. The gas was dried by passing it through a tube containing $CaSO_4$ as a drying agent. The heating rate (β) was varied from 2 to 12°C min^{-1}. These conditions were applied to all types of stearic acid mentioned in Section 2.1.
(b) *Varying N_2 flow rate*: The heating rate was maintained at 6°C min^{-1} throughout the experiment. The N_2 flow rate was varied from 50 to 1000 ml min^{-1}. Preliminary experiments suggested that all the samples showed the same general trend. Results are, therefore, reported in this study for stearic acid B as this represents the type of sample used in pharmaceutical formulations.

For all the runs, rising temperature experiments were conducted in the temperature range from ambient to 350°C. An open, 110 μl platinum crucible with a cross-sectional area (∀) of 0.294 cm^2 was used to contain the sample and an empty platinum crucible of equivalent size was used as a reference. The sample sizes were in the range of 6.99 to 7.38 mg.

Plots of $\ln k$ vs. $1/T$ were constructed using the data collected from the DTG (derivative thermogravimetric) plot. The coefficient of evaporation per unit area (k) has units of mg min^{-1} cm^{-2} and the temperature (T) is in Kelvin. The data needed to produce such

Table 1
The experimental data obtained form the DTG plot of stearic acid A at the heating rate of 2°C min^{-1} under an atmosphere of dry N_2

Temperature/K	1/*T*/ (K^{-1})	DTG signal=d*w*/d*t*/(mg min^{-1})	*k*/(mg min^{-1} cm^{-2})	ln *k*
415	0.00241	0.00180	0.0061	−5.097
417	0.00240	0.00215	0.0073	−4.917
419	0.00239	0.00246	0.0084	−4.783
423	0.00236	0.00340	0.0116	−4.460
—	—	—	—	—
—	—	—	—	—
—	—	—	—	—
515	0.00194	0.48470	1.6498	0.501

a plot for stearic acid A is recorded in Table 1. Similar data were obtained for the other two stearic acid samples (B and C). The activation energy of each experiment at a specific heating rate or flow rate can be easily determined from the slope of this plot.

3. Results and discussion

3.1. Vary the heating rate

Fig. 1 represents the TG, DTA and DTG plots of stearic acid B at the heating rate of 10°C min^{-1} as an example. It can be seen that the evaporation takes place after the completion of melting. The DTA signal shows two distinct endotherms on account of the melting at a lower temperature and vaporization at a higher temperature. The onset of the evaporation process could be easily noticed from the DTG plot, where the signal begins to depart from its baseline. It should be noted that the melting process can be seen as a small perturbation in the DTG plot. This is probably caused by a buoyancy effect due to the escape of air as bubbles from the newly formed liquid. The DTG signal returns to the baseline after the initial perturbation.

The melting point peak temperature, the evaporation peak temperature along with the heating rate of stearic acid determined from the DTA peak temperature are reported in Table 2. The heating rate used in this study does not seem to significantly effect the melting points. However, the peak temperatures of the evaporation endotherms increased when the heating rates increase. It should be noted that the amount of impurity present, such as palmitic acid (having the melting point of 63–64°C), obviously lowers the melting temperature of the material.

Table 3 records the sample entity, β, E_{act}, correlation coefficient (R^2), and the determined temperature range. The values of E_{act} are calculated from the DTG data as set out in Section 2.3. The values of E_{act} for stearic acids A, B and C are in the 95.1–101.1, 93.7–98.7 and 89.0–92.4 kJ mol^{-1} range, respectively. From this result, it is obvious that the purer the material, the higher is the value of E_{act}.

Table 2
The observed DTA peak temperatures for stearic acids A, B, and C showing melting and evaporation endotherms

β/(°C min^{-1})	Stearic acid A [a]/°C		Stearic acid B [a]/°C		Stearic acid C [a]/°C	
	DTA_1 [b]	DTA_2 [c]	DTA_1 [b]	DTA_2 [c]	DTA_1 [b]	DTA_2 [c]
2	71.1	242.2	68.3	243.3	57.4	236.2
4	71.9	259.4	69.3	257.8	57.7	250.3
6	71.7	267.8	69.7	267.4	58.7	259.3
8	73.0	274.0	70.4	274.0	59.3	263.1
10	71.5	281.0	71.0	279.6	59.5	271.6
12	73.5	286.0	70.2	278.9	59.5	274.9

[a] Peak temperatures are reported due to the shape of the peak and the nature of the baseline (Fig. 1).
[b] Melting endotherm.
[c] Evaporation endotherm.

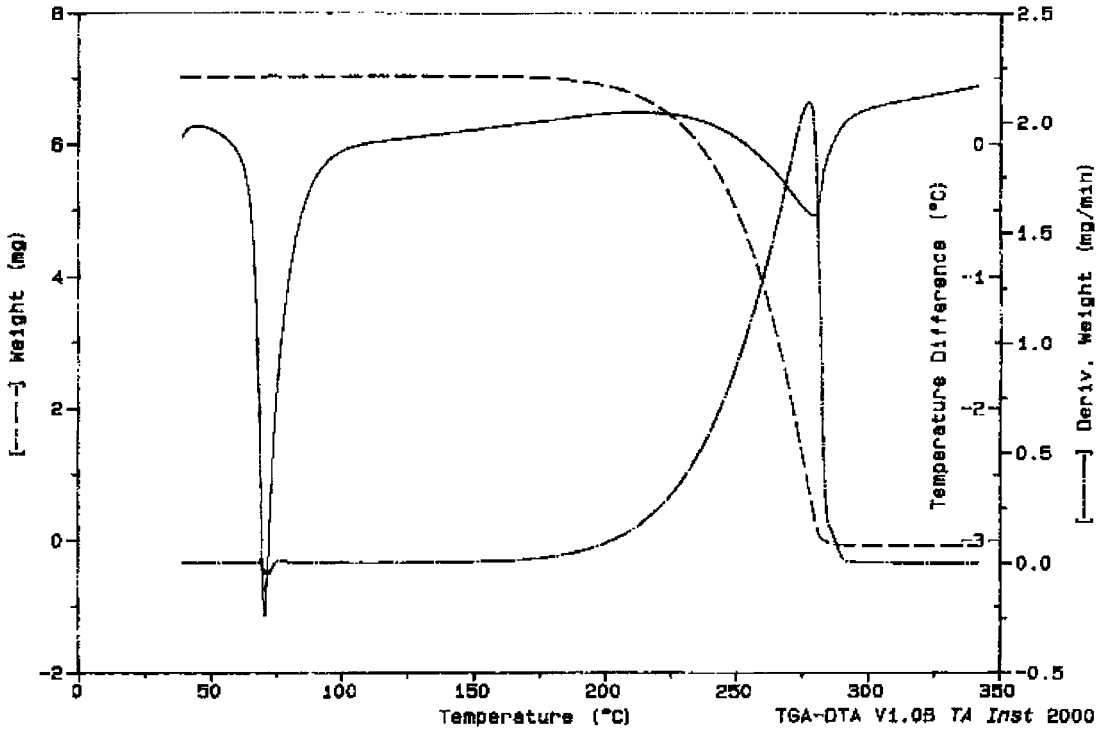

Fig. 1. A plot of TG, DTA, and DTG signals for stearic acid B at the heating rate of 10°C min^{-1} under an atmosphere of dry N_2.

Fig. 2 shows the plot of E_{act} vs. the heating rate for all stearic acids being investigated. The value of E_{act} of the material decreases when the heating rate increases. This obviously results from the shift of the evaporation process to a higher temperature region when the heating rate rises.

3.2. Varying N_2 flow rate

For this set of experiments, the variation of E_{act} of vaporization with the flow rate of the purge gas was studied. Table 4 sets out the DTA peak temperature for stearic acid B studied at different flow rates. The effects of flow rate on E_{act}, R^2, and the determined temperature range for the evaporation experiments are shown in Table 5. The values of E_{act} are in the range of 87.0 to 91.9 kJ mol^{-1} calculated from data collected over the temperature range from 200°C to the peak temperature in the DTG plots. The flow rates and the E_{act} values have an approximately logarithmic relationship with an R^2 of 0.880.

3.3. The evaporation process

The process of evaporation is endothermic and a schematic diagram is shown in Fig. 3. The energy transition, on going through the kinetic pathway, involves an E_{act} as noted in the diagram. The thermodynamic quantity (ΔH_{vap}) is only concerned with the energy difference between the initial (liquid) and the final (gas) states, and is independent of the pathway. It can be seen that $E_{act} > \Delta H_{vap}$, and in the lower limit

$$E_{act} \rightarrow \Delta H_{vap}$$

In fact, ΔH_{vap} value as calculated from Eq. (2) is 115.7 kJ mol^{-1} at 109°C, but drops to 81.6 kJ mol^{-1} at 280°C, the temperature region in which the majority of vaporization proceeds in our thermoanalytical experiments. This latter value can be compared with a range of E_{act} values from 87.0 to 101.1 kJ mol^{-1} observed from our various evaporation experiments, and the general ideas portrayed in Fig. 3 are seen to hold.

Table 3
β, E_{act}, correlation coefficient (R^2), and the determined temperature range for stearic acids A, B, and C

β/(°C min^{-1})	E_{act}/(kJ mol^{-1})	R^2	Temperature range/K
Stearic acid A			
2	101.1	0.998	415–515
4	100.8	0.997	413–529
6	99.0	0.008	413–539
8	97.5	0.998	433–545
10	97.3	0.997	431–551
12	95.1	0.998	441–555
Stearic acid B			
2	98.1	0.996	413–515
4	96.5	0.999	423–529
6	96.3	0.999	421–539
8	94.7	0.999	435–545
10	94.1	0.998	443–551
12	93.7	0.999	433–549
Stearic acid C			
2	92.4	0.996	413–505
4	91.8	0.997	415–519
6	91.0	0.997	431–529
8	90.0	0.996	425–537
10	89.7	0.997	439–541
12	89.0	0.997	435–547

Table 4
The observed DTA peak temperatures for stearic acid B at varying N_2 flow rate showing melting and evaporation endotherm[s]

N_2 Flow rate/(ml min^{-1})	DTA_1 [b]/°C	DTA_2 [c]/°C
50	69.6	268.2
100	69.7	267.4
150	69.7	266.1
200	69.7	266.0
250	69.6	265.5
300	69.5	264.8
400	70.0	265.5
600	69.5	263.1
1000	69.0	263.1

[a] Peak temperatures are reported due to the shape of the peak and the nature of the baseline (Fig. 1).
[b] Melting endotherm.
[c] Evaporation endotherm.

Nevertheless, the actual coefficient of vaporization (k), at 210°C, varies with the heating rate over a small range (Fig. 4). There is a larger variation of k with the flow rate at this temperature as seen in Fig. 5, but it must be pointed out that the variation in the flow rate covers a large range (from 50 to 1000 ml min^{-1}).

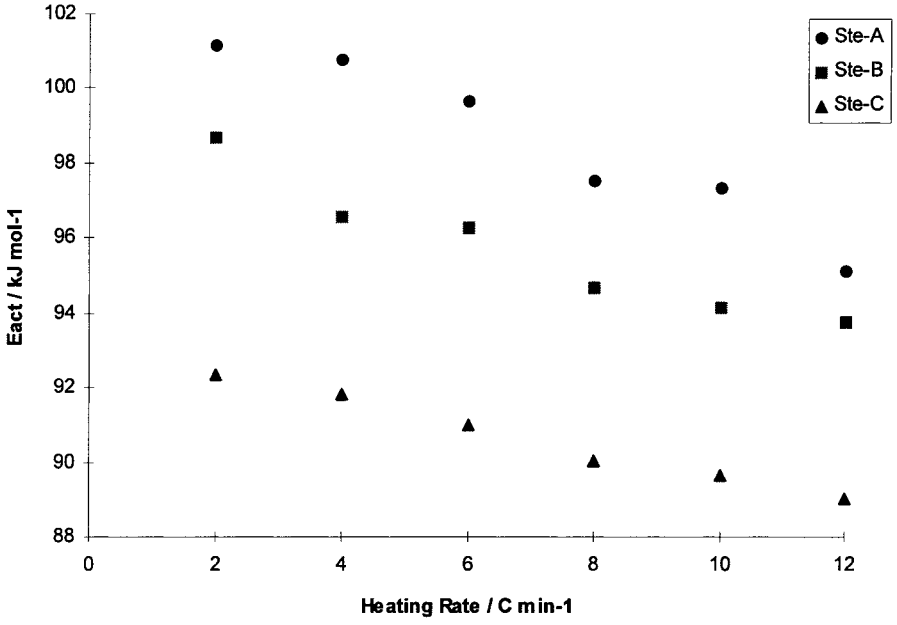

Fig. 2. A plot of the heating rate vs. E_{act} for stearic acid (●) A, (■) B, and (▲) C.

Table 5
The N_2 flow rate, E_{act}, correlation coefficient (R^2), and the determined temperature range for stearic acid B

N_2 Flow rate/ (ml min^{-1})	E_{act}/ (kJ mol^{-1})	R^2	Temperature range/K
50	91.9	0.998	473–539
100	90.3	0.998	473–539
150	89.1	0.997	473–537
200	88.4	0.996	473–537
250	89.5	0.998	473–535
300	88.1	0.997	473–535
400	88.4	0.997	473–535
600	87.0	0.996	473–533
1000	87.1	0.997	473–531

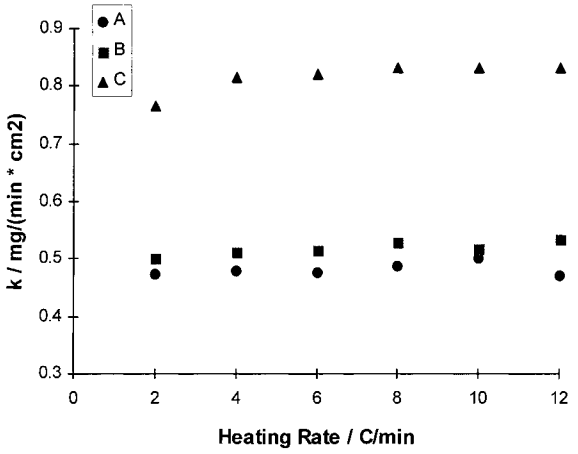

Fig. 4. Plots of the heating rate vs. k at 210°C for stearic acid (●) A, (■) B, and (▲) C.

The DTA signals per unit mass (in this case, per mg) can also be examined. A plot of the evaporation peak area (in °C min mg^{-1}) vs the heating rate for stearic acids A, B, and C is portrayed in Fig. 6(a) and a similar plot of peak height is shown in Fig. 6(b). It can be seen that the plot gives the largest peak area at 6–8°C min^{-1}. The size of the peak area at the lower heating rate is rendered more difficult to assess and this is the probable reason for the variation at low heating rate of the peak area. However, the magnitude of the peak height is seen to increase as the heating is increased. The negative sign in Fig. 6(b) is used because the transition is endothermic. This arises since the evaporation peak is sharper and confined to a shorter temperature range as the heating rate is increased. As the mass of the sample varies during the experiment, one cannot use such data to estimate the enthalpy. However, beyond the heating rate of

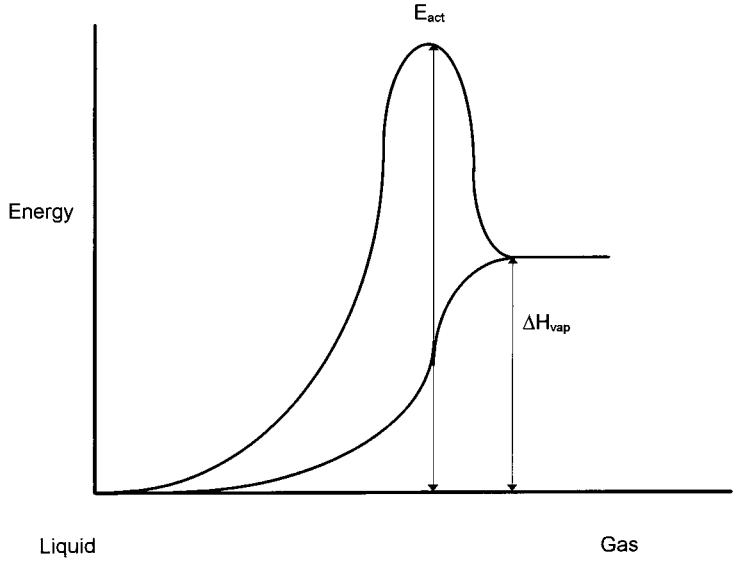

Fig. 3. A schematic diagram showing an energy transition from liquid to gas.

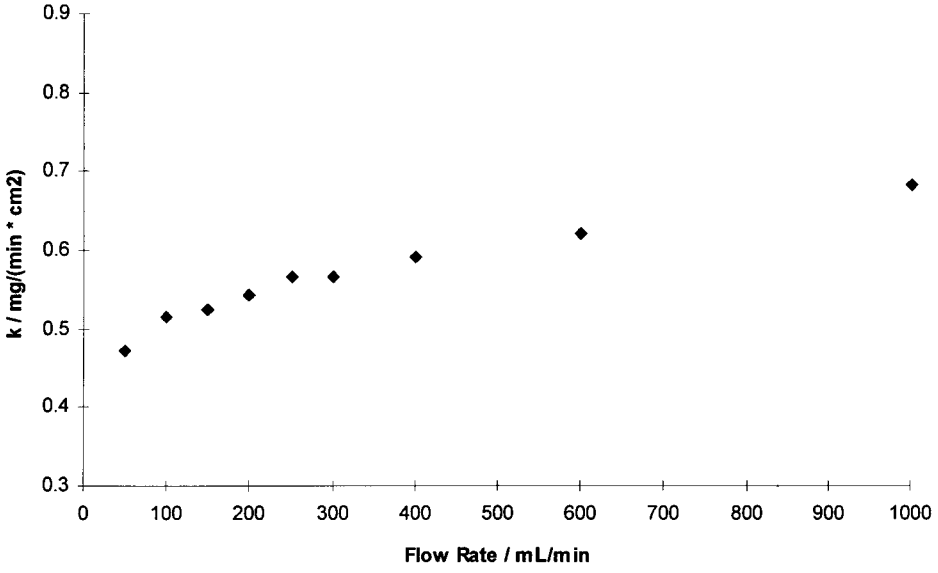

Fig. 5. A plot of N_2 flow rate vs. k at 210°C for stearic acid B.

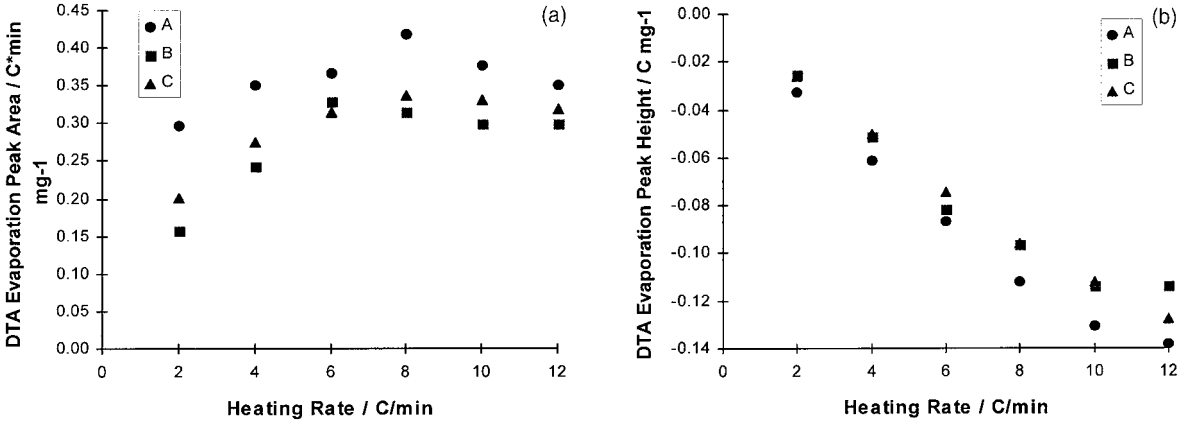

Fig. 6. (a) Plots of the heating rate vs. DTA evaporation peak area per mg sample for stearic acid (●) A, (■) B, and (▲) C. (b) Plots of the heating rate vs. DTA evaporation peak height per mg sample for stearic acid (●) A, (■) B, and (▲) C.

6°C min^{-1}, there is a possibility of using the data to estimate the quantity of stearic acid present.

A plot of DTA signals per mg sample vs. the flow rate for stearic acid B, when the heating rate was kept constant at 6°C min^{-1}, is shown in Fig. 7. An N_2 flow rate of 100 ml min^{-1} yields the largest peak area (in °C min mg^{-1}) and the largest magnitude of peak height (in °C mg^{-1}). However, the variation in peak height is almost negligible at a flow rate between 50 to 300 ml min^{-1}.

For the stearic acid evaporation experiments, the optimum heating rate is 6–8°C min^{-1} under a N_2 flow rate of 100 ml min^{-1}.

3.4. Comparison of equilibrium vapor pressure with the evaporation process

At equilibrium, we have the Clausius–Clapeyron equation:

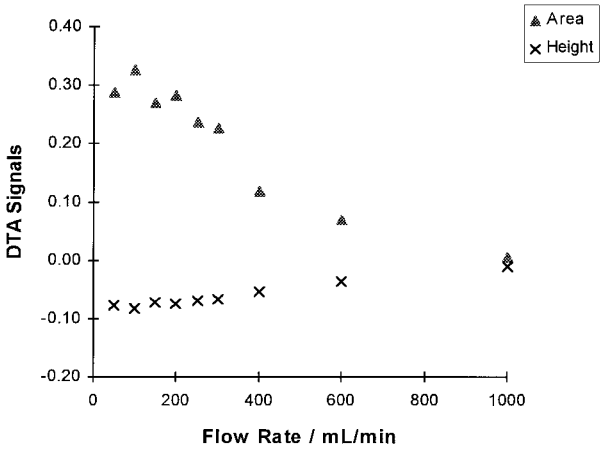

Fig. 7. Plots of N_2 flow rate vs. DTA evaporation peak area (▲, in °C min) and peak height (×, in °C) per mg sample for stearic acid B in experiments performed at a heating rate of 6°C min^{-1}.

$$\ln P_s = G - \frac{\Delta H_{vap}}{RT} \tag{4}$$

where G is a constant of integration. Using Eqs. (3) and (4) over the range of the thermal analysis experiments, we have

$$RT \ln P_s = RTG - \Delta H_{vap}$$

and

$$RT \ln k = RT \ln Z - E_{act}$$

In the limit, as we approach equilibrium conditions, $E_{act} \rightarrow \Delta H_{vap}$ (see Fig. 3). At any specific temperature, T_i, however, we have

$$\ln P_s - \ln k = G - \ln Z$$

$$\ln P_s = \ln k + D \tag{5}$$

where D is a constant.

The $\ln P_s$ can be calculated from Eq. (1) and $\ln k$ was determined from the experimental data as shown in Table 1 as an example. A plot of $\ln P_s$ vs. $\ln k$ (for stearic acid A, at a heating rate of 6°C min^{-1}) at corresponding temperatures (473–539 K) produces a linear relationship as shown in Fig. 8. This demonstrates that the relationship predicted in Eq. (5) holds experimentally.

The relationships drawn up here are experimentally based. The attempts we make here to correlate E_{act} and ΔH_{vap} stem directly from the basic relationship portrayed in Fig. 3 and found in most physical chemistry textbooks.

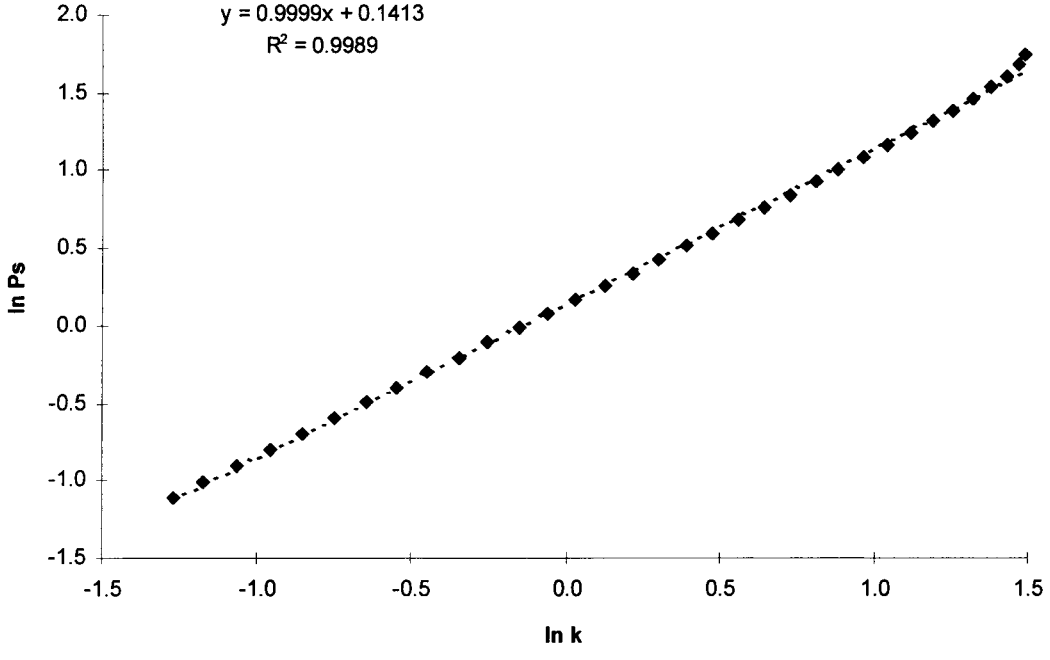

Fig. 8. A plot of ln k (at β=6°C min^{-1} in N_2 flow rate at 100 ml min^{-1}) vs. $\ln P_s$ in the temperature range of 473 to 539 K.

References

[1] R.M. Stephenson, S. Malamowski, Handbook of the Thermodynamics of Organic Compounds, Elsevier, New York, 1987, p. 428.
[2] V. Majer, V. Svoboda, J. Pick, Heats of Vaporization of Fluids, Elsevier, Amsterdam, 1989, p. 27.
[3] J.C. Boylan, J. Cooper, Z.T. Chowhan, W. Lund, A. Wade, R.F. Weir, B.J. Yates, Handbook of Pharmaceutical Excipients, The American Pharmaceutical Association and The Pharmaceutical Society of Great Britain, 1986, p. 298.
[4] The United States Pharmacopoeia 23 and The National Formulary 18, United States Pharmacopeial Convention Inc., 1995, p. 2310.
[5] S. Budavari (Ed.), The Merck Index, 11th edn., Merck & Co. Inc., Rahway, NJ, 1989, p. 1386.